

Chemical Biology | Hot Paper |

Selective Inhibition of Aggregation and Toxicity of a Tau-Derived Peptide using Its Glycosylated Analogues

Moran Frenkel-Pinter,^[a] Michal Richman,^[b] Anna Belostozky,^[b] Amjaad Abu-Mokh,^[a] Ehud Gazit,^{*[a]} Shai Rahimipour,^{*[b]} and Daniel Segal^{*[a]}

Abstract: Protein glycosylation is a ubiquitous post-translational modification that regulates the folding and function of many proteins. Misfolding of protein monomers and their toxic aggregation are the hallmark of many prevalent diseases. Thus, understanding the role of glycans in protein aggregation is highly important and could contribute both to unraveling the pathology of protein misfolding diseases as well as providing a means for modifying their course for therapeutic purposes. Using β -O-linked glycosylated variants of

the highly studied Tau-derived hexapeptide motif VQIVYK, which served as a simplified amyloid model, we demonstrate that amyloid formation and toxicity can be strongly attenuated by a glycan unit, depending on the nature of the glycan itself. Importantly, we show for the first time that not only do glycans hinder self-aggregation, but the glycosylated peptides are capable of inhibiting aggregation of the non-modified corresponding amyloid scaffold.

Introduction

Protein glycosylation, the abundant enzyme-directed site-specific process that attaches glycans to proteins, regulates the folding and function of many proteins. Two main types of protein glycosylation are known in the secretory pathway, classified according to the nature of the linkage between the core region of the glycan and the modified residue in the protein: N-glycosylation, which occurs on asparagine residue, and O-glycosylation, which occurs on a serine or threonine residue.^[1] Many monosaccharides, including *N*-acetylgalactosamine (GalNAc), *N*-acetylglucosamine (GlcNAc) and galactose are involved in the O-glycosidic bond formation in nature.^[2] In addition, many proteins within the nucleus, cytoplasm and mitochondria are dynamically glycosylated with GlcNAc on their serine or threonine residues through a β -glycosidic linkage. This process, termed *O*-GlcNAcylation, is highly competitive with phosphorylation on the same or adjacent amino acids.^[3]

Various studies have shown that glycosylation has many implications on protein folding.^[4] Glycan chains attached to nascent proteins are believed to be important for promoting their

correct folding and maintaining the structural integrity, thus preventing protein aggregation. Protein aggregation is the hallmark of protein misfolding diseases, which are characterized by the self-assembly of monomers of certain proteins into toxic oligomers and fibrils composed of β -sheet structures, termed amyloids.^[5] These conditions, include amyloid plaques of A β peptides and neurofibrillary tangles (NFTs)—aggregates of hyperphosphorylated Tau protein in Alzheimer's disease (AD) and amyloid aggregates composed of the prion protein in Creutzfeldt–Jakob disease (CJD).^[5b,6] Notably, various amyloid forming proteins including Tau and the prion protein are glycosylated. Thus, understanding the effect of glycans on protein self-assembly, which appears to be an initial key step in the pathology of these amyloidogenic diseases, can both contribute to unraveling the pathology of these diseases as well as provide means for modifying the course of these diseases for therapeutic purposes.

Glycan chains attached to proteins often hinder their aggregation rate by modulating the conformational properties of the protein involved.^[7] Specifically, several studies have suggested that glycosylated peptides favor conformations in which the peptide backbone bends away from the bulky glycosylation site.^[8] For example, the Tau protein in the brain of AD patients is less *O*-GlcNAcylated and more hyperphosphorylated than in healthy individuals. Hyperphosphorylation of Tau has been causally linked to its propensity to form toxic amyloid aggregates, while *O*-GlcNAcylation of Tau has been shown to reduce its aggregation rate.^[7c,m] Indeed, inhibiting the enzyme β -*N*-acetylglucosaminidase (OGA) that removes *O*-GlcNAc from proteins, increased Tau *O*-GlcNAcylation in tauopathy model mice, decreased formation of Tau aggregates and reduced neuronal cell loss.^[7c] Despite these findings which imply a role for glycans in reducing protein aggregation, a sys-

[a] M. Frenkel-Pinter, A. Abu-Mokh, Prof. E. Gazit, Prof. D. Segal
Department Molecular Microbiology and Biotechnology, and
the Interdisciplinary Sagol School of Neurosciences
George S. Wise Faculty of Life Sciences, Tel-Aviv University
Tel Aviv 69978 (Israel)
E-mail: dsegal@post.tau.ac.il
ehudg@post.tau.ac.il

[b] Dr. M. Richman, A. Belostozky, Prof. S. Rahimipour
Department of Chemistry, Bar-Ilan University
Ramat-Gan 5290002 (Israel)
E-mail: rahimis@biu.ac.il

Supporting information for this article can be found under <http://dx.doi.org/10.1002/chem.201504950>.

tematic study comparing the effect of different glycans on amyloid formation has not been performed, except for few reports utilizing a prion-derived amyloid scaffold.^[7k,l,n]

Importantly, in nature both glycosylated and non-glycosylated variants of a glycoprotein coexist in the cellular environment. Thus, they may interact with each other and impact their respective aggregation. The studies mentioned above have all addressed only the effect of the glycan on the self-assembly of the peptide/protein, yet none explored a possible effect of a glycopeptide on the corresponding non-glycosylated amyloid scaffold as likely occurs in the cellular milieu. Notably and interestingly, as opposed to well controlled protein glycosylation, the non-enzymatic process of protein glycation, which occurs mainly on lysine residues, was reported to often accelerate amyloid fibril formation.^[9]

Most glycosylated proteins harbor large N- or O-linked glycan trees, which are very difficult to synthesize and conjugate to a full-length protein of interest. To simplify this system, we have studied the effect of various monosaccharides on the aggregation propensity of a Tau-derived peptide, Ac-SVQIVYK-NH₂ (corresponding to residues 305–311 in the full-length, 441 amino acids long Tau protein), as an amyloid scaffold. This 7aa peptide is based on the short fragment VQIVYK (also known as PHF6), which was shown to be critical for Tau aggregation into oligomers and formation of NFTs.^[10] We employed Ac-SVQIVYK-NH₂ as a simplified amyloidogenic model peptide, bearing in mind that it is not known to carry glycans in vivo. We decorated this scaffold with various glycans, including β -linked galactose (Gal), glucosamine (GlcN) and *N*-acetylglucosamine (GlcNAc), on a single glycosylation site on the serine residue. We examined in vitro the effect of the various glycans on the self-assembly propensity of the modified PHF6 and on the inhibitory properties of the corresponding glycosylated peptides towards amyloidogenic aggregation of non-modified native PHF6.

Our results indicate that glycosylation dramatically decreased self-fibrillogenesis of Ac-SVQIVYK-NH₂, and in addition rendered it remarkably efficient in inhibiting the aggregation of the non-modified PHF6. Importantly, the effect of glycosylation appears to be strongly dependent on the nature of the glycan itself.

Results and Discussion

ThS analysis reveals that glycosylation of the PHF6-derived peptide inhibit its amyloidogenic aggregation

To explore whether glycosylation of PHF6 scaffold modulates its aggregation propensity, an extended version of it was glycosylated on an upstream Ser with different glycans, including Gal, GlcN and GlcNAc (Table 1 and Figure 1). All the glycans had the same β -glycosidic bond conformation to exclude effect of anomericization of the C1 carbon. GlcN and GlcNAc differ only in their charge due to the free amino group of GlcN at the C2 position, whereas Gal lacks the amino group at C2 position and differs in the orientation of a single hydroxyl group at the C4 position. The sequences of all peptides em-

ployed in this study and their abbreviations are shown in Table 1. All peptides were synthesized using the solid-phase peptide synthesis.

To examine the ability of glycosylated PHF6-derived peptides to form amyloid structures, the peptides were incubated in the presence of heparin and their aggregation kinetics was followed by the thioflavin S (ThS) fluorescence assay.^[11] The results suggested that while PHF6 and the non-modified 7aa peptide aggregate rapidly within less than 30 min (Figure 2 and Figure S1 in the Supporting Information), glycosylation of the 7aa scaffold with either Gal, GlcN and GlcNAc drastically reduced its propensity to aggregate (Figure 2).

Table 1. Sequences of the PHF6-based model peptides used in this study.	
Peptide	Sequence
PHF6	[Ac-VQIVYK-NH ₂]
7aa	[Ac-SVQIVYK-NH ₂]
7aa-Gal	[Ac-S(β Gal)VQIVYK-NH ₂]
7aa-GlcN	[Ac-S(β GlcN)VQIVYK-NH ₂]
7aa-GlcNAc	[Ac-S(β GlcNAc)VQIVYK-NH ₂]

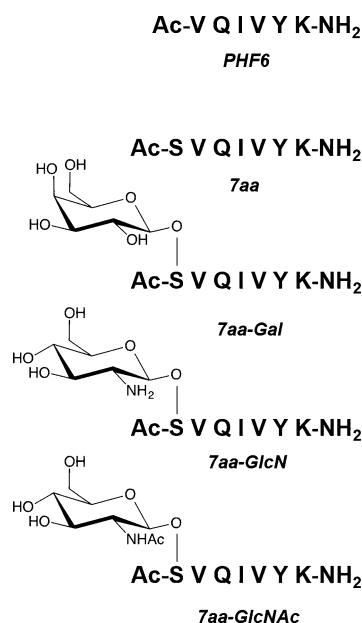


Figure 1. Chemical structure of PHF6-derived peptides used in the study. Seven amino acid long, Ac-SVQIVYK-NH₂, extended versions of PHF6, were synthesized, and glycosylated on their serine residues with various glycan moieties, including galactose (Gal), glucosamine (GlcN) and *N*-acetyl glucosamine (GlcNAc).

The various glycans have distinct effects on the secondary structure of the amyloid scaffold

In order to study the effect of the different glycans on the secondary structure of PHF6-derived peptide, circular dichroism (CD) spectroscopy was used. In the absence of heparin, all PHF6-derived peptides exhibited a large negative peak near

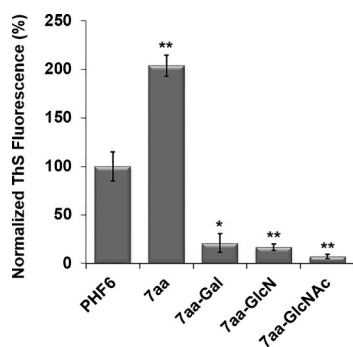


Figure 2. ThS analysis of self-assembly of PHF6-derived peptides. Representative normalized end-point ThS fluorescence obtained after 60 min incubation of 100 μM of the 7aa-derived peptides in the presence of 1 μM heparin at 25 $^{\circ}\text{C}$. The ThS fluorescence value observed from PHF6 signal is considered as 100% aggregation. The Student's t-test analysis showed *, $P < 0.05$, **, $P < 0.01$.

200 nm, indicating a random coil conformation (Figure 3 A).^[12] Addition of heparin to the non-glycosylated PHF6-derived peptides caused secondary structural changes over time from a random coil to a β -sheet conformation, characterized by a strong positive peak around 195 nm and a negative peak around 220 nm (Figure 3 B). Glycosylation of the 7aa peptide with GlcN drastically inhibited the structural transformation from random coil to β -sheet structure, while conjugation with Gal only partially inhibited this transformation. In contrast, glycosylation of the 7aa peptide with GlcNAc had no effect on the secondary structure of the peptide (Figure 3 B).

TEM analysis of PHF6-derived peptides reveals that glycans alter the morphology of the resulting amyloid aggregates

In order to study the effect of the glycans on the morphology of the PHF6-derived peptide, TEM analysis was performed on the samples of the various modified and non-modified peptides. Figure 4 shows the TEM images of the peptides after being incubated with heparin for 25 min. PHF6 and the non-modified 7aa peptide formed clustered large fibrils, which were helically twisted around their central axis. PHF6 fibrils were all straight, as opposed to the fibrils formed by the non-modified 7aa peptide, which were a mixture of straight and moderately curved fibrils. In contrast, only very few fibrils were observed for the 7aa-GlcN peptide (Figure 4), in agreement with the results of the ThS and CD analyses. The 7aa-GlcNAc peptide, which exhibited a β -sheet conformation in the CD analysis (Figure 3 B), also formed fibrillar structures similar to those formed by PHF6, although fewer fibrils were detected and various amorphous structures were observed. These TEM results are in good agreement with the ThS results, indicating the lower amyloidogenic propensity of 7aa-GlcNAc to self-aggregate (Figure 2). The 7aa-Gal peptide, which exhibited a mixture of random coil and β -sheet structures in the CD spectra (Figure 3 B), formed large clustered fibrils that were much more curved in their morphology than those formed by PHF6 and the non-modified 7aa peptide (Figure 4). The highly curved fibril morphology of 7aa-Gal peptide may account for

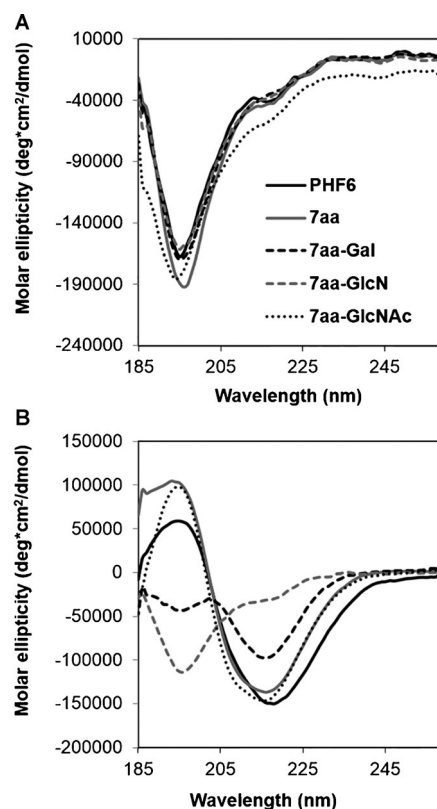


Figure 3. CD spectra of the various peptides in the presence or absence of heparin. The secondary structure of 7aa-derived peptides incubated for 3 h at 25 $^{\circ}\text{C}$ in the: A) absence, or B) presence of heparin.

its weak ThS signal, since thioflavin-based fluorophores favor binding to specific amyloid structures.^[11,13]

Collectively, these results demonstrate that various glycans, linked by a β -glycosidic bond to the Tau-derived PHF6 amyloidogenic scaffold, reduce the self-aggregation propensity of the glycosylated PHF6-derived peptides and alter their second-

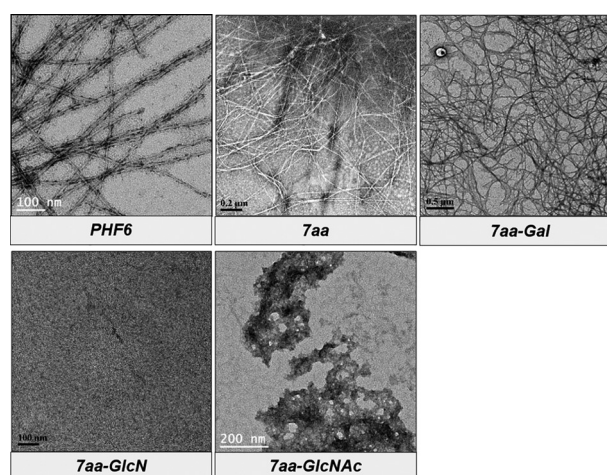


Figure 4. TEM images of self-assembled 7aa-based peptides. TEM images were taken after the peptide analogues (100 μM) were allowed to aggregate at 25 $^{\circ}\text{C}$ for 25 min following initiation of aggregation by the addition of heparin (1 μM).

dary conformation and aggregate morphology (Figure 3, Figure 4). Our findings indicate that the effect of glycosylation on self-aggregation of the amyloid scaffolds is strongly dependent on the nature of the glycan itself, as the different glycans used in our study (β -linked Gal, GlcN and GlcNAc) demonstrated different effects on amyloidogenic self-aggregation propensity of the Tau-derived peptide. Comparable results have been reported for a prion-derived amyloid scaffold using α -mannose, α -galactose, α -GalNAc, α -GlcNAc, β -GlcNAc, or β -GalNAc.^[7k,l,n]

Various elements within the glycan ring, such as the orientation of a single hydroxyl group at the C4 of the glycan and the anomeric position of the glycan, have been shown to affect the self-aggregation propensity of glycopeptides.^[7k,l,n] In our study we found that 7aa-GlcN is not aggregative, as opposed to 7aa-GlcNAc and 7aa-Gal. This is most probably due to the presence of the charged amino group on C2 of the glycan ring, which likely induces a charge repulsion between the PHF6 scaffold and thus decreases its self-assembly propensity.

Notably, two of the glycans used in this study that hindered self-aggregation of the PHF6-scaffold, namely β -Gal and β -GlcNAc, were previously reported to slow down in vitro fibrillogenesis of other amyloid model peptides, including the prion-derived peptide, the 26 amino acids long model α -helical hairpin peptide and the α -helical hairpin peptide (α -helix/turn/ α -helix).^[7a,k-n] To the best of our knowledge, our study is the first to explore the impact of charged β -GlcN on amyloidogenic aggregation propensity, and to demonstrate its high inhibitory effect.

Glycosylation of the PHF6-derived peptide attenuates its cytotoxicity

One of the most important basic mechanisms of neuronal dysfunction in amyloid neurodegeneration is the cytotoxic interaction of amyloid aggregates with the cell plasma membrane.^[14] We have recently demonstrated that Ac-PHF6 permeates PC12 cells and dose-dependently reduces their viability.^[15] In order to determine the effect of PHF6-derived peptides on cell viability, PC12 cells were incubated for 24 h with the peptides (10 μ M) and their survival was determined by the MTT assay. Figure 5 shows that Ac-PHF6 and its 7aa non-glycosylated analogue induced a significant toxicity towards PC12 cells. Glycosylation of the PHF6-derived peptide (7aa) with Gal and GlcNAc did not alter its toxicity, while its conjugation with GlcN significantly ($P < 0.001$) reduced the toxicity (Figure 5).

These results correlate well with the CD and TEM results, where only 7aa-GlcN did not generate β -sheet-rich fibrillar structures (Figure 3B and Figure 4).

Our results may shed light on the effect of the various glycans on PHF6-induced cytotoxicity. We observed a positive strong correlation between aggregation propensity and cytotoxicity. The non-aggregative 7aa-GlcN demonstrated very low toxicity, whereas the non-modified 7aa and the two remaining 7aa-derived glycopeptides, which were more aggregative, were also more cytotoxic.

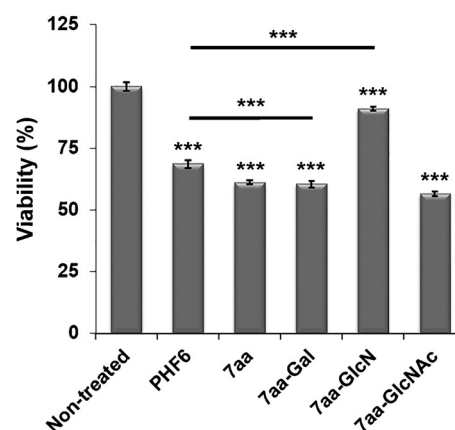


Figure 5. The effect of PHF6-derived peptides on the viability of PC12 cells. PC12 cells were treated for 24 h with 10 μ M 7aa-derived peptides and cell viability was measured using the MTT assay. The Student's t-test analysis showed ***, $P < 0.001$.

Table 2 summarizes the effect of the different glycans on both the structure and toxicity of the PHF6-derived peptides. Collectively, these results suggest that effect of glycosylation on toxicity could be best predicted by the CD and TEM analyses and not by the ThS binding capability.

PHF6-derived glycosylated peptides inhibit the aggregation rate of native PHF6

To explore a possible inhibitory effect of the glycosylated peptides on PHF6 aggregation, we compared the aggregation of PHF6 in the presence or absence of the peptides listed in Table 1, at a 1:1 or 10:1 molar ratio, in favor of PHF6 (Figure 6). Co-incubation of 100 μ M of PHF6 with 100 μ M of the non-modified 7aa peptide (Figure 6A) caused a significant increase

Table 2. Effect of the different glycans on the self-assembly and toxicity of PHF6-derived peptides.

Peptide	Secondary structure ^[a]	Aggregate abundance and morphology ^[b]	Toxicity [%]
PHF6	β -sheet	many straight, helically twisted fibrils	31.5 \pm 1.7
7aa	β -sheet	many straight and few moderately curved, helically twisted fibrils	38.8 \pm 0.8
7aa-Gal	mixture of β -sheet and random coil	many curved fibrils	39.5 \pm 1.4
7aa-GlcN	random coil	very few short fibrils	9.1 \pm 0.8
7aa-GlcNAc	β -sheet	few curved fibrils, few amorphous structures	43.4 \pm 0.9

[a] Aggregation following addition of heparin. [b] According to the TEM analysis.

of the total ThS fluorescence signal, as expected. Incubation of PHF6 (100 μM) with the lower concentration of the non-modified 7aa peptide (10 μM , Figure 6A) resulted in similar ThS fluorescence signal as PHF6 alone, suggesting that it had no inhibitory effect on the aggregation of PHF6. In contrast, incubation of PHF6 with various 7aa-glycosylated peptides (Figure 6B–D), markedly decreased the aggregation rate of PHF6 (Table 3). Notably, for all glycopeptides, an effect of their dose on inhibition of PHF6 aggregation was observed (Figure 6B–D). Despite their inhibitory effect on the aggregation rate of PHF6, the glycosylated peptides mostly did not lead to a decrease in the ThS fluorescence signal at the end of the experiment (Figure 6E). As a control, we verified that supplementing PHF6

with PHF6 molecule itself increased its aggregation as measured by ThS Fluorescence (Figure S2 in the Supporting Information).

Table 3. Aggregation rate following co-incubation of PHF6 with the various peptides at a 1:1 molar ratio.

Peptide	Average aggregation rate (normalized to PHF6)
PHF6	1
7aa	1.3 \pm 0.18
7aa-Gal	0.41 \pm 0.03
7aa-GlcN	0.41 \pm 0.07
7aa-GlcNAc	0.59 \pm 0.06

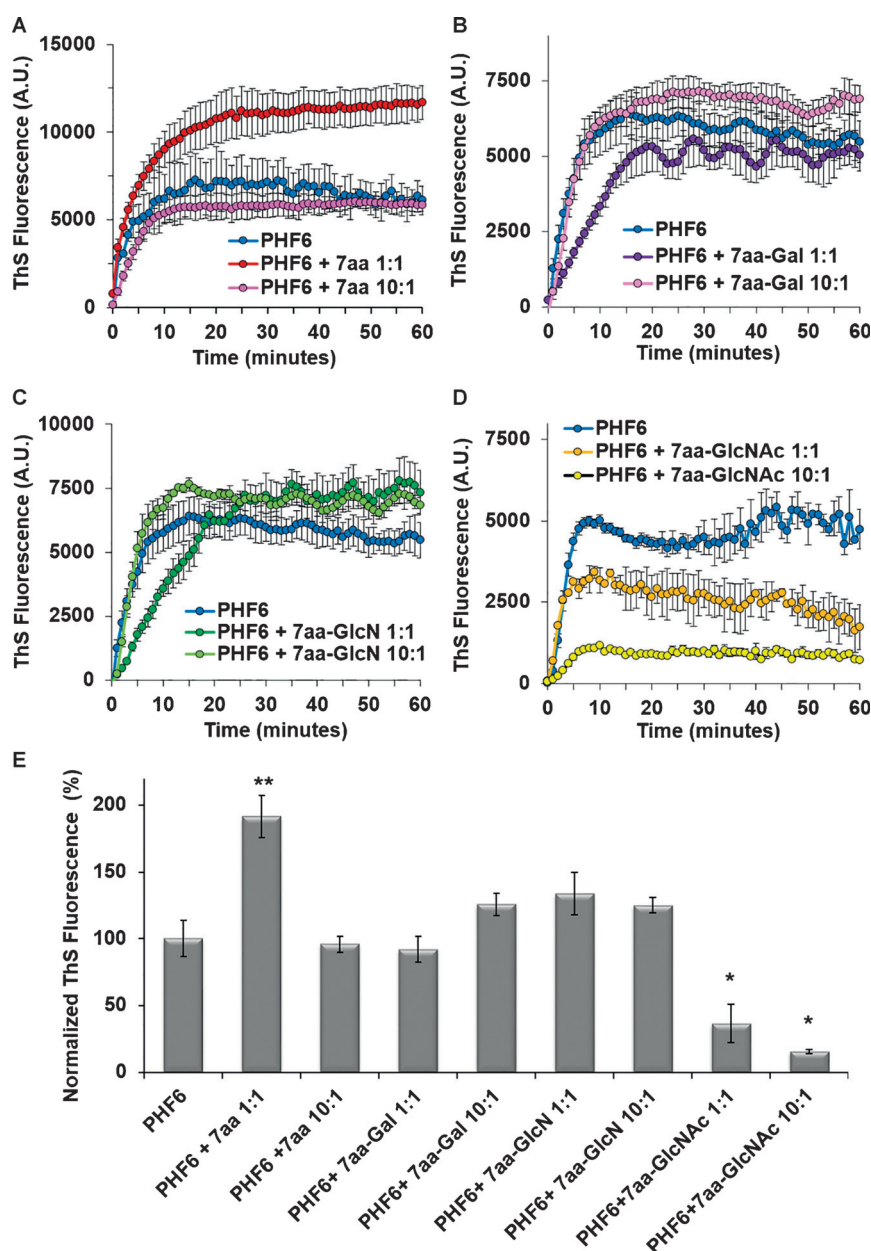


Figure 6. The effect of the 7aa-derived peptides on PHF6 aggregation. Kinetic ThS fluorescence measurements of PHF6 (at 100 μM , 1 μM heparin) in the presence or absence of: A) non-modified 7aa peptide, B) 7aa-Gal, C) 7aa-GlcN, and D) 7aa-GlcNAc, at 10:1 and 1:1 molar ratio (PHF6/inhibitory peptide). End-point ThS fluorescence recordings of (A–D) are shown in (E). The end-point ThS fluorescence signal was normalized to PHF6 signal. The Student's t-test analysis showed *, $P < 0.05$, **, $P < 0.01$.

The effect of the parent 7aa peptide and its glycosylated analogues on PHF6 aggregation was also studied by TEM (Figure S3 in the Supporting Information). The results confirmed that incubation of non-modified 7aa peptide and its glycosylated analogues with PHF6 had little or no effect on the amount of generated fibrils. The results also demonstrate that increased aggregation occurs upon co-incubation of PHF6 with the higher concentration of the non-modified 7aa peptide (Figure S3), in accordance with ThS fluorescence results (Figure 6A). Yet, the morphology of some of the fibrils, resulting in these co-incubation experiments, appears to be different from that of PHF6 alone. Cell viability experiments revealed that the nontoxic 7aa-GlcN does not alter PHF6-induced toxicity towards the PC12 cell line (Figure S4 in the Supporting Information).

While hindrance of self-aggregation of amyloid scaffolds by glycans has been previously reported, to the best of our knowledge, this study demonstrates for the first time that glycosylated peptides are capable of inhibiting the aggregation of a non-modified corresponding amyloid scaffold. Importantly, this inhibitory effect appears to be strongly dependent on the nature of the glycan itself. We note that inhibition of aggregation by glycopeptides should be also examined in other experimental setups, such as the fast flow microfluidic system.^[16] We hypothesize that the glycopeptides were able to compete for interaction with native PHF6 monomers and intercalate with them, leading to less interaction between the PHF6 monomers themselves. This inhibitory effect is of special importance since in cellular environment both glycosylated and non-glycosylated variants of a given protein coexist and may interact with each other, thus impacting their respective aggregation and toxicity. We speculate that rational conjugation of glycans to peptides induces steric hindrance that could be used as a novel way for robust and specific inhibition of amyloidogenic aggregation, thus expanding the biotechnological applications of glycopeptides for therapeutic purposes.^[17]

Ho et al.^[7] proposed that glycosylation interferes with amyloid formation during the nucleation step. This was based on the observation that Prion-derived glycopeptides aggregated once seeded with the wild-type prion-derived peptide fibrils. When considering the self-interactions of the glycosylated peptides or their interactions with PHF6 it is worthwhile to note that glycans can form a variety of noncovalent bonds with protein residues.^[18] The hydroxyl groups of carbohydrates can form hydrogen bonds with amino acids such as lysine, arginine, histidine, aspartic acid and glutamic acid. On the other hand, the hexose ring can adopt a conformation in which several of its carbon atoms are in a cluster that can form energetically favorable CH- π stacking interactions with parallel aligned aromatic rings of, for example, tyrosine, phenylalanine or tryptophan.^[18,19] It is thus possible that the glycans in our glycoscaffolds interact with the lysine or with the tyrosine, located in the PHF6 core itself, disrupting the tight packing interactions that mediate protein self-assembly into fibrils. The aromatic tyrosine residue in PHF6 was previously shown to be crucial for its aggregation.^[20] Given the crucial role of aromatic residues in amyloid formation,^[21] interference with (π - π) stack-

ing interactions by glycopeptides may have bearing on drug design.

Conclusions

Glycosylation of proteins play a key role in their structure, function, and stability, and has been implicated in various diseases involving toxic aggregation of the misfolded proteins. Our results demonstrate that amyloid formation can be attenuated by a single glycan unit. Nevertheless, the effect of glycosylation appears to be also strongly dependent on the nature of the glycan itself. We demonstrated that in addition to hindrance of self-aggregation by glycans, glycopeptides are capable of inhibiting the aggregation of non-modified corresponding amyloid scaffolds.

We believe that our results may shed new light on the complex mechanism of protein aggregation *in vivo*, where several differently modified glycopeptides coexist simultaneously inside the cell environment. Our results provide valuable information for the design of glycopeptide mimetics as possible therapeutic agents for protein misfolding diseases.

Experimental Section

Peptide synthesis

All chemicals and reagents were of analytical grade. Fluorenylmethoxycarbonyl (Fmoc)-protected amino acid derivatives, and all other reagents for solid-phase peptide synthesis were purchased either from Novabiochem (San Diego CA, USA) or GL Bio-chem (Shanghai, China). Unless otherwise stated, all other chemicals were obtained from Sigma-Aldrich (Rehovot, Israel). Peptides were purified to homogeneity (> 98% purity) by RP-HPLC and analyzed by mass spectrometry. Fmoc-Ser(β -Ac₃GlcNHBOC)-OH and Fmoc-L-Ser(β -Ac₄Gal)-OH were synthesized as previously described.^[22]

Fmoc-Ser(β -Ac₃GlcNHAc)-OH

Fmoc-Ser(β -Ac₃GlcNHBOC)-OH was treated with 50% TFA in DCM for 2 h. The solvents were concentrated *in vacuo*, and the crude product was then dissolved in CH₂Cl₂ and acetylated using 4 equiv of acetic anhydride and 2 equiv of DIPEA in DCM for 2 h. The solvents were evaporated by reduced pressure and the crude material was then purified by preparative RP-HPLC.

Synthesis of glycosylated peptides

VQIVYK-NH₂ was synthesized automatically (Vantage, AAPPTec, Louisville, KY) on Rink-Amide resin using solid-phase peptide synthesis and employing the common Fmoc strategy.^[23] The peptide-bound resin was either acetylated following Fmoc deprotection, using a solution of acetic anhydride (10 equiv) and DIPEA (20 equiv) in NMP for 1 h, or coupled overnight with either Fmoc-Ser(β -Ac₃GlcNHBOC)-OH, Fmoc-L-Ser(β -Ac₄Gal)-OH, Fmoc-Ser(β -Ac₃GlcNHAc)-OH (3 equiv) or Fmoc-L-Ser(OtBU)-OH in the presence of PyBOP (3 equiv), HOAt (3 equiv) and *N*-methylmorpholine (NMM, 9 equiv) in *N*-methylpyrrolidone (NMP). Following incorporation of the amino acids, the terminal Ser was acetylated following Fmoc deprotection, using a solution of acetic anhydride (10 equiv) and DIPEA (20 equiv) in NMP for 1 h. Finally, the O-acetyl groups of the glycosylated Ser were removed with 20% hydrazine hydrate in

MeOH (2×2.5 h), and the final products were released from the resin and totally deprotected using a mixture of TFA/triethylsilane/H₂O (95:2.5:2.5 v/v) for 2 h. All the glycosylated peptides were then precipitated with cold diethyl ether, purified by preparative HPLC and analyzed by HRMS. HRMS *m/z*: calcd for C₃₈H₆₂N₈O₁₀ (Ac-VQIVYK-NH₂): 790.9465, found 791.4660. HRMS *m/z*: calcd for C₄₁H₆₈N₁₀O₁₁ (Ac-SVQIVYK-NH₂): 877.0390, found 877.5140. HRMS *m/z*: calcd for C₄₇H₇₈N₁₀O₁₆ (Ac-S(βGal)VQIVYK-NH₂): 1039.1796, found 1039.5674. HRMS *m/z*: calcd for C₄₇H₇₉N₁₁O₁₅ (Ac-S(βGlcN)VQIVYK-NH₂): 1038.1949, found 1038.5832. HRMS *m/z*: calcd for C₄₉H₈₁N₁₁O₁₆ (Ac-S(βGlcNAc)VQIVYK-NH₂): 1080.2315, found 1080.5936.

ThS fluorescence aggregation assay

In order to ensure the monomeric state of the peptides, the lyophilized peptides were pretreated for 10 min with 1,1,1,3,3,3-hexafluoroisopropanol (HFIP) at 37 °C. Following the dissolution, the solvent was evaporated using a SpeedVac or a stream of nitrogen. Immediately prior to the experiment, the peptides were dissolved in water and sonicated for 5 min. The concentration of each peptide was then determined (calculated according to ϵ_{280} of 1490 M⁻¹cm⁻¹) and adjusted to 1 mM concentration as the stock solution. A stock solution of Thioflavin S (ThS, 2 mM, Sigma–Aldrich, Rehovot, Israel) and heparin (1 mM, Sigma–Aldrich, Rehovot, Israel) were prepared in 20 mM MOPS (pH 7.2). For self-assembly experiments, stock solutions were diluted in 100 μ L wells of a 96-well black plate so that the final mixture contained 100 μ M of the peptide/glycopeptide and 100 μ M ThS in 20 mM MOPS. For experiments involving inhibition of PHF6 aggregation, PHF6 (100 μ M) was incubated in the wells of a 96-well black plate with or without the inhibitory peptides (10 or 100 μ M) in MOPS buffer (20 mM) in the presence of ThS (100 μ M). Immediately prior to experiment, heparin (1 μ M) was added to initiate peptide aggregation, as previously described.^[10a,24] As a control, the PHF6 peptide was supplemented instead of the inhibitory peptide. Kinetic fluorescence data were collected at 25 °C in triplicate or quadruplicate using Infinite M200 microplate fluorescence reader (Tecan, Switzerland), with measurements taken at 1 min intervals for 60 min. Excitation and emission wavelengths were 440 and 490 nm, respectively. All of the experiments were repeated 3–4 times to ensure reproducibility. For calculation of average aggregation rate (Table 3), kinetic data from the first five minutes of the experiment were used and the corresponding aggregation curves were fitted to a linear trend line (linear regression), from which the slope was calculated.

Circular dichroism (CD) analysis

To analyze the secondary structure of the various peptides, each peptide (100 μ M) was incubated in the absence or presence of 1 μ M heparin for 3 h at 25 °C. Prior to measurements, samples were diluted 2.5 times and placed in a 0.1 mm cuvette. CD spectra were then recorded on a Chirascan spectrometer in the range of 185–260 nm, and the background was subtracted from the CD spectra.

Transmission electron microscopy (TEM)

For self-assembly experiments, each peptide (100 μ M) was allowed to aggregate for 25 min at 25 °C in the presence of heparin (1 μ M). For PHF6 inhibition experiments, PHF6 (100 μ M) was incubated with heparin under the same conditions in the presence or absence of increasing concentrations of the inhibitory peptides (molar ratio of 10:1 and 1:1, PHF6/inhibitory peptide). Samples

(10 μ L) were placed for 2 min on 400-mesh copper grids covered with carbon-stabilized Formvar film (Electron Microscopy Sciences (EMS), Hatfield, PA). Excess fluid was removed, and the grids were negatively stained with 2% uranyl acetate solution (10 μ L) for 2 min. Finally, excess fluid was removed and the samples were viewed by a JEM-1400 TEM (JEOL) or Tecnai G2 TEM (FEI), operated at 80 kV.

Cell culture experiments

Pheochromocytoma (PC12) cells were grown in low-glucose Dulbecco's modified Eagle medium (DMEM) supplemented with 10% horse serum and 5% fetal bovine serum (FBS), L-glutamine, penicillin, and streptomycin in a 5% CO₂, humidified atmosphere, at 37 °C. To study the effect of the various peptides on the viability of PC12 cell cultures, cells were seeded at a cell density of 1×10⁴ cells per 100 μ L medium, into each well of a 96-well plate. Fresh medium containing the peptides (10 μ M) was then added to the wells and incubation was continued for an additional 24 h. Cell viability was then determined by the 3-(4,5-dimethylthiazol-2-yl)-2,5-diphenyltetrazolium bromide (MTT) assay. For studying a possible inhibitory effect of the various peptides on PHF6-induced toxicity, fresh medium containing PHF6 (10 μ M) together with increasing concentrations of the inhibitory peptide (molar ratio of 10:1 and 1:1, PHF6/inhibitory peptide) were added to the cells. Control wells received the equivalent amount of water and MOPS (20 mM) were considered as 100% cell viability. Cells were incubated for an additional 24 h, and cell viability was then determined by the MTT assay. Each experiment was performed in quadruplicate and repeated at least three times.

Statistics

Student's t-test was performed for evaluating statistical significance of the observed differences (*p*-value < 0.05 was considered to be statistically different).

Acknowledgements

We are grateful to the members of the D.S., E.G. and S.R. research groups for fruitful discussions, and especially to Dr. Marina Chemerovski from S.R.'s group.

Keywords: amyloid formation · glycopeptides · glycosylation · PHF6 · protein and peptide aggregation

- [1] A. Varki, J. D. Esko, K. J. Colley, in *Essentials of Glycobiology*, 2nd ed. (Eds.: A. Varki, R. D. Cummings, J. D. Esko, H. H. Freeze, P. Stanley, C. R. Bertozzi, G. W. Hart, M. E. Etzler), Cold Spring Harbor, **2009**.
- [2] R. S. Haltiwanger, J. B. Lowe, *Annu. Rev. Biochem.* **2004**, *73*, 491–537.
- [3] G. W. Hart, Y. Akimoto, in *Essentials of Glycobiology*, 2nd ed. (Eds.: A. Varki, R. D. Cummings, J. D. Esko, H. H. Freeze, P. Stanley, C. R. Bertozzi, G. W. Hart, M. E. Etzler), Cold Spring Harbor, **2009**.
- [4] a) D. Shental-Bechor, Y. Levy, *Proc. Natl. Acad. Sci. USA* **2008**, *105*, 8256–8261; b) D. Shental-Bechor, Y. Levy, *Curr. Opin. Struct. Biol.* **2009**, *19*, 524–533; c) J. L. Price, D. Shental-Bechor, A. Dhar, M. J. Turner, E. T. Powers, M. Gruebele, Y. Levy, J. W. Kelly, *J. Am. Chem. Soc.* **2010**, *132*, 15359–15367; d) J. L. Price, E. K. Culyba, W. Chen, A. N. Murray, S. R. Hanson, C. H. Wong, E. T. Powers, J. W. Kelly, *Biopolymers* **2012**, *98*, 195–211; e) J. J. Caramelo, A. J. Parodi, *FEBS Lett.* **2015**, *589*, 3379–3387; f) A. Tannous, G. B. Pisoni, D. N. Hebert, M. Molinari, *Semin. Cell Dev. Biol.* **2015**, *41*, 79–89.

- [5] a) A. Pastore, P. Temussi, *J. Phys. Condens. Matter* **2012**, *24*, 244101; b) T. P. Knowles, M. Vendruscolo, C. M. Dobson, *Nat. Rev. Genet.* **2014**, *15*, 384–396.
- [6] a) J. F. Díaz-Villanueva, R. Diaz-Molina, V. Garcia-Gonzalez, *Int. J. Mol. Sci.* **2015**, *16*, 17193–17230; b) J. Ma, F. Wang, *Essays Biochem.* **2014**, *56*, 181–191.
- [7] a) M. Broncel, J. A. Falenski, S. C. Wagner, C. P. Hackenberger, B. Kokschi, *Chem. Eur. J.* **2010**, *16*, 7881–7888; b) F. C. Liang, R. P. Chen, C. C. Lin, K. T. Huang, S. I. Chan, *Biochem. Biophys. Res. Commun.* **2006**, *342*, 482–488; c) S. A. Yuzwa, X. Shan, M. S. Macauley, T. Clark, Y. Skorobogatko, K. Vosseller, D. J. Vocadlo, *Nat. Chem.* **2012**, *8*, 393–399; d) D. F. Wyss, J. S. Choi, J. Li, M. H. Knoppers, K. J. Willis, A. R. Arulanandam, A. Smolyar, E. L. Reinherz, G. Wagner, *Science* **1995**, *269*, 1273–1278; e) S. R. Hanson, E. K. Culyba, T. L. Hsu, C. H. Wong, J. W. Kelly, E. T. Powers, *Proc. Natl. Acad. Sci. USA* **2009**, *106*, 3131–3136; f) V. Kayser, N. Chennamsetty, V. Voynov, K. Forrer, B. Helk, B. L. Trout, *Biotechnol. J.* **2011**, *6*, 38–44; g) A. Taraboulos, M. Rogers, D. R. Borchelt, M. P. McKinley, M. Scott, D. Serban, S. B. Prusiner, *Proc. Natl. Acad. Sci. USA* **1990**, *87*, 8262–8266; h) P. M. Rudd, A. H. Merry, M. R. Wormald, R. A. Dwek, *Curr. Opin. Struct. Biol.* **2002**, *12*, 578–586; i) C. J. Bosques, B. Imperiali, *Proc. Natl. Acad. Sci. USA* **2003**, *100*, 7593–7598; j) P. M. Rudd, M. R. Wormald, D. R. Wing, S. B. Prusiner, R. A. Dwek, *Biochemistry* **2001**, *40*, 3759–3766; k) C. Lin, E. H. Chen, L. Y. Lee, R. L. Hsu, F. Y. Luh, L. L. Yang, C. F. Chou, L. D. Huang, C. C. Lin, R. P. Chen, *Carbohydr. Res.* **2014**, *387*, 46–53; l) C. C. Ho, L. Y. Lee, K. T. Huang, C. C. Lin, M. Y. Ku, C. C. Yang, S. I. Chan, R. L. Hsu, R. P. Chen, *Proteins* **2009**, *76*, 213–225; m) C. H. Yu, T. Si, W. H. Wu, J. Hu, J. T. Du, Y. F. Zhao, Y. M. Li, *Biochem. Biophys. Res. Commun.* **2008**, *375*, 59–62; n) P. Y. Chen, C. C. Lin, Y. T. Chang, S. C. Lin, S. I. Chan, *Proc. Natl. Acad. Sci. USA* **2002**, *99*, 12633–12638; o) R. Roytman, L. Adler-Abramovich, K. S. Kumar, T. C. Kuan, C. C. Lin, E. Gazit, A. Brik, *Org. Biomol. Chem.* **2011**, *9*, 5755–5761.
- [8] a) B. Imperiali, K. W. Rickert, *Proc. Natl. Acad. Sci. USA* **1995**, *92*, 97–101; b) C. J. Bosques, S. M. Tschampel, R. J. Woods, B. Imperiali, *J. Am. Chem. Soc.* **2004**, *126*, 8421–8425; c) S. E. O’Conner, B. Imperiali, *Chem. Biol.* **1998**, *5*, 427–437; d) S. Dziadek, C. Griesinger, H. Kunz, U. M. Reinscheid, *Chem. Eur. J.* **2006**, *12*, 4981–4993; e) L. Kirmarsky, O. Prakash, S. M. Vogen, M. Nomoto, M. A. Hollingsworth, S. Sherman, *Biochemistry* **2000**, *39*, 12076–12082; f) D. M. Coltart, A. K. Royyuru, L. J. Williams, P. W. Glunz, D. Sames, S. D. Kuduk, J. B. Schwarz, X. T. Chen, S. J. Danishefsky, D. H. Live, *J. Am. Chem. Soc.* **2002**, *124*, 9833–9844; g) F. Corzana, J. H. Busto, G. Jimenez-Oses, M. Garcia de Luis, J. L. Asensio, J. Jimenez-Barbero, J. M. Peregrina, A. Avenoza, *J. Am. Chem. Soc.* **2007**, *129*, 9458–9467; h) C. R. Ellis, W. G. Noid, *J. Phys. Chem. B* **2014**, *118*, 11462–11469; i) D. N. Hebert, L. Lamriben, E. T. Powers, J. W. Kelly, *Nat. Chem. Biol.* **2014**, *10*, 902–910.
- [9] C. Iannuzzi, G. Irace, I. Sirangelo, *Front. Mol. Biosci.* **2014**, DOI: 10.3389/fmolb.2014.00009.
- [10] a) M. von Bergen, P. Friedhoff, J. Biernat, J. Heberle, E. M. Mandelkow, E. Mandelkow, *Proc. Natl. Acad. Sci. USA* **2000**, *97*, 5129–5134; b) B. Bulic, M. Pickhardt, B. Schmidt, E. M. Mandelkow, H. Waldmann, E. Mandelkow, *Angew. Chem. Int. Ed.* **2009**, *48*, 1740–1752; *Angew. Chem.* **2009**, *121*, 1772–1785.
- [11] M. Biancalana, S. Koide, *Biochim. Biophys. Acta* **2010**, *1804*, 1405–1412.
- [12] N. J. Greenfield, *Nat. Prot.* **2007**, *1*, 2876–2890.
- [13] L. Bousset, L. Pieri, G. Ruiz-Arlandis, J. Gath, P. H. Jensen, B. Habenstein, K. Madiona, V. Olieric, A. Bockmann, B. H. Meier, R. Melki, *Nat. Commun.* **2013**, *4*, 2575.
- [14] a) M. Bucciantini, D. Nosi, M. Forzan, E. Russo, M. Calamai, L. Pieri, L. Formigli, F. Quercioli, S. Soria, F. Pavone, J. Savistchenko, R. Melki, M. Stefani, *FASEB J.* **2012**, *26*, 818–831; b) Y. Zhang, R. McLaughlin, C. Goodyer, A. LeBlanc, *J. Cell Biol.* **2002**, *156*, 519–529; c) M. Bucciantini, E. Giannoni, F. Chiti, F. Baroni, L. Formigli, J. Zurdo, N. Taddei, G. Ramponi, C. M. Dobson, M. Stefani, *Nature* **2002**, *416*, 507–511; d) M. Andreassen, N. Lorenzen, D. Otzen, *Biochim. Biophys. Acta* **2015**, *1848*, 1897–1907.
- [15] A. Belostozky, M.Sc. Thesis, Bar-Ilan University, Ramat-Gan, **2014**.
- [16] M. H. Horrocks, L. Tosatto, A. J. Dear, G. A. Garcia, M. Iljina, N. Cremades, M. Dalla Serra, T. P. Knowles, C. M. Dobson, D. Klenerman, *Anal. Chem.* **2015**, *87*, 8818–8826.
- [17] a) I. García, A. Sanchez-Iglesias, M. Henriksen-Lacey, M. Grzelczak, S. Penades, L. M. Liz-Marzan, *J. Am. Chem. Soc.* **2015**, *137*, 3686–3692; b) M. C. Rodriguez, M. Cudic, *Methods Mol. Biol.* **2013**, *1081*, 107–136; c) E. Zacco, J. Hutter, J. L. Heier, J. Mortier, P. H. Seeberger, B. Lepenies, B. Kokschi, *ACS Chem. Biol.* **2015**, *10*, 2065–2072; d) D. Yuan, J. Shi, X. Du, N. Zhou, B. Xu, *J. Am. Chem. Soc.* **2015**, *137*, 10092–10095; e) Y. Kamiya, T. Satoh, K. Kato, *Curr. Opin. Struct. Biol.* **2014**, *26*, 44–53; f) Y. F. Liu, Z. Y. Sun, P. G. Chen, Z. H. Huang, Y. Gao, L. Shi, Y. F. Zhao, Y. X. Chen, Y. M. Li, *Bioconjugate Chem.* **2015**, *26*, 1439–1442.
- [18] E. K. Culyba, J. L. Price, S. R. Hanson, A. Dhar, C. H. Wong, M. Gruebele, E. T. Powers, J. W. Kelly, *Science* **2011**, *331*, 571–575.
- [19] a) F. A. Quijcho, *Curr. Top. Microbiol. Immunol.* **1988**, *139*, 135–148; b) F. A. Quijcho, *Annu. Rev. Biochem.* **1986**, *55*, 287–315; c) V. Voynov, N. Chennamsetty, V. Kayser, B. Helk, K. Forrer, H. Zhang, C. Fritsch, H. Heine, B. L. Trout, *PLoS ONE* **2009**, *4*, e8425; d) V. Spiwok, P. Lipovova, T. Skalova, E. Vondrackova, J. Dohnalek, J. Hasek, B. Kralova, *J. Comput. Aided Mol. Des.* **2006**, *19*, 887–901.
- [20] a) H. Inouye, D. Sharma, W. J. Goux, D. A. Kirschner, *Biophys. J.* **2006**, *90*, 1774–1789; b) K. Sogawa, R. Okuda, Y. In, T. Ishida, T. Taniguchi, K. Minoura, K. Tomoo, *J. Biochem.* **2012**, *152*, 221–229.
- [21] a) E. Gazit, *FASEB J.* **2002**, *16*, 77–83; b) Y. Porat, Y. Mazor, S. Efrat, E. Gazit, *Biochemistry* **2004**, *43*, 14454–14462; c) P. Marek, A. Abedini, B. Song, M. Kanungo, M. E. Johnson, R. Gupta, W. Zaman, S. S. Wong, D. P. Raleigh, *Biochemistry* **2007**, *46*, 3255–3261; d) S. M. Tracz, A. Abedini, M. Driscoll, D. P. Raleigh, *Biochemistry* **2004**, *43*, 15901–15908; e) O. S. Makin, E. Atkins, P. Sikorski, J. Johansson, L. C. Serpell, *Proc. Natl. Acad. Sci. USA* **2005**, *102*, 315–320; f) G. G. Tartaglia, A. Cavalli, R. Pellarin, A. Caffisch, *Protein Sci.* **2005**, *14*, 2723–2734; g) S. Jones, J. Manning, N. M. Kad, S. E. Radford, *J. Mol. Biol.* **2003**, *325*, 249–257; h) G. G. Tartaglia, A. Cavalli, R. Pellarin, A. Caffisch, *Protein Sci.* **2004**, *13*, 1939–1941.
- [22] L. Motiei, S. Rahimpour, D. A. Thayer, C. H. Wong, M. R. Ghadiri, *Chem. Commun.* **2009**, 3693–3695.
- [23] E. Atherton, R. C. Sheppard, *Solid Phase Peptide Synthesis: A Practical Approach*, Oxford University Press, Oxford, **1989**.
- [24] a) M. von Bergen, S. Barghorn, L. Li, A. Marx, J. Biernat, E. M. Mandelkow, E. Mandelkow, *J. Biol. Chem.* **2001**, *276*, 48165–48174; b) K. Zhao, G. Ippolito, L. Wang, V. Price, M. H. Kim, G. Cornwell, S. Fulencheck, G. A. Breen, W. J. Goux, S. R. D’Mello, *J. Neurosci. Res.* **2010**, *88*, 3399–3413; c) C. L. Moore, M. H. Huang, S. A. Robbenolt, K. R. Voss, B. Combs, T. C. Gambelin, W. J. Goux, *Biochemistry* **2011**, *50*, 10876–10886.

Received: December 9, 2015

Published online on February 18, 2016